

MICROSTRUCTURAL IMAGE ANALYSES OF MILD CARBON STEEL SUBJECTED TO A RAPID CYCLIC HEAT TREATMENT

Orhadahwe Thomas Aghogho¹, Adeleke Adekunle Akanni², Aweda Jacob Olayiwola¹,
Ikubanni Peter Pelumi³, Odusote, Jamiu Kolawole²

¹ Mechanical Engineering Department, University of Ilorin, Ilorin, Nigeria

Received 25 February 2019

² Materials and Metallurgical Engineering Department,
University of Ilorin, Ilorin, Nigeria

Accepted 31 July 2019

³ Mechanical Engineering Department, Landmark University, Omu Aran, Nigeria
E-mail: ikubanni.peter@lmu.edu.ng

ABSTRACT

The study is focused on using an image analysis to explain the effects of several cycles of rapid heat treatment on the microstructure of 0.213 wt. % carbon steel. The samples examined are subjected to a diffusional heat treatment followed by several cycles of a rapid heat treatment. The process of the diffusional heat treatment involves heating the samples from an ambient temperature to 850°C in an electric muffle furnace for 56 min and then quenching in running water. In order to improve further the mechanical properties of the heat treated samples, they are subjected to several cycles of rapid heating. Each cycle comprises preheating the furnace to 900°C prior to the samples charging. The treated samples are subjected to a microstructural examination using optical microscopy followed by an image analysis using Image J software. The mechanical properties of the heat treated samples are characterized through ultimate tensile, hardness and impact tests. The results reveal that the grain size decreases from 1.07 µm in the control sample to 0.79 µm in the three-cycle sample and increases to 0.86 µm in the four-cycle one. It is also observed that the two-cycle sample shows the highest ductility (15356.3 N/mm²) and the lowest ultimate strength (833.375 N/mm²). This implies that the two-cycle rapid heat treatment is required for grain refinement in mild carbon steel.

Keywords: rapid heating, microstructure, image analysis, martensite, quenching.

INTRODUCTION

The specific mechanical properties of the metal products are basic requirements for their application [1]. These properties can be obtained along different strengthening mechanisms which act together during the deformation process. The heat treatment [2] is one of these mechanisms because it affects [3, 4] the products strength and toughness. The properties considered improve with the grain size refining but the mechanism of the process is not entirely clear for martensitic steels [5]. According to Muszka et al. [1] the procedure to strengthen a metal depends on its chemical composition, its deformation history and the resulting microstructure. Tejas [6] assumes that the grain refinement provides a different orientation of the grains preventing thus dislocations, crack initiations and failures. This in turn

strengthens the material. The grain refinement can be achieved by rapid heating [7]. Grange [8] advances the possibility of austenite grains refinement by shortening the austenite cycle. This can be achieved by subjecting the steel to a rapid heat treatment which involves heating at a fast rate to its austenitic temperature and immediate quenching without soaking. It is argued whether the steel soaking at this temperature is necessary. It is worth noting that the process of a rapid austenitizing treatment saves time, costs and minimizes the steel oxidation and decarburization. The minimization of the austenite grain growth leads to the formation of fine grains in the heat treated product.

Dabkowski and Porter [9] suggest that the rapid heat treatment spanning between 5 min and 30 min has to be immediately followed by quenching. According to Twiggs et al. [10] a heating rate above 20°C/min should

be considered a fast one. In fact the rapid heat treatment involves the use of fast heating rates. The process generates a surface of properties which are distinctly different from those of the initial microstructure obtained through a conventional or a diffusional heat treatment [11]. The literature data shows that the temperature and the time of the heat treatment process affect the mechanical properties. It is so because the increase of the heating rate leads to smaller, equiaxed grains of increased hardness, yield and fatigue strength [12]. Grange [8] states that one or two cycles of a rapid heat treatment would produce ultra-fine mild steel grains of increased strength and toughness. However, there is no verification of this claim. There are several studies on the application of a rapid heat treatment of other steel grades [9 - 13]. There are also several investigations on thermal cycling [14 - 17] but none of them focuses on the effect of the rapid cyclic heat treatment of mild steel. Lv et al. [18] accept that the traditional route of a cyclic heat treatment involves preheating and repeated quenching and tempering which is time consuming.

The method used in this study applies several cycles of rapid heating and quenching which decreases the heat treatment demands in respect to time, energy and cost. This study verifies also the claim of Grange [8] that one or two cycles of a rapid heat treatment would provide strength and toughness in mild steel. The study is aimed at the determination of the exact number of the cycles required to result in toughness and ductility increase in the mild steel subjected to a quenching heat treatment.

In addition, the study uses an image analysis to explain the microstructural behavior of the heat treated steel. It is a process of acquiring quantitative information on the microstructural parameters of a material including size, solidity, porosity and circularity. There are several software programs designed to carry out this analysis. They refer to Amira, Consol multiphysics and Image J [19]. Despite the increasing application of the image analysis, there are only a few references [19, 20]. Image J software is used in the present investigation and aimed at elucidating the effect of the rapid cyclic heat treatment on mild steel microstructure.

EXPERIMENTAL

Sample preparation

The elemental composition of the AISI 1021 steel sample was obtained using optical electron spectrometry. The data obtained is presented in Table 1. It was found that the steel sample contained 0.213 wt. % of carbon which qualified it as mild steel [21, 22].

The material used was cut and machined to the required tests dimensions with the aid of a lathe machine. The samples were then labeled for the various cycles of the heat treatment as shown in Table 2.

Initial diffusional heat treatment

The diffusional (conventional) heat treatment procedure for producing martensitic steels involves slow heating to austenite and rapid cooling of austenized specimen in a quenching medium [23]. All samples

Table 1. Chemical composition (wt. %) of the steel sample.

C	Si	S	P	Mn	Ni	Al	W
0.213	0.252	0.030	0.028	0.779	0.131	0.292	<0.0001
Cr	Mo	V	Cu	Nb	B	Ti	Fe
0.138	0.020	0.030	0.336	0.014	0.001	0.009	97.700

Table 2. Sample identification tag based on various cycle of treatment.

Sample	Control (A)	One cycle (B)	Two cycle (C)	Three cycles (D)	Four cycles (E)
Heat treatment	Diffusional heat treatment only	Diffusional and one cycle of rapid heat treatment	Diffusional and two cycles of rapid heat treatment	Diffusional and three cycles of rapid heat treatment	Diffusional heat treatment and four cycles of rapid heat treatment

were subjected to a diffusional heat treatment which involved slow heating from a room temperature to the austenite one (852 °C) and soaking for 10 min [24, 25]. The austenized steel samples were then rapidly cooled using tap water. The heating and the cooling rates were determined electronically with a thermocouple connected to the data logger.

Cyclic rapid heat treatment

The electric muffle furnace was preheated to 900°C to increase the heating rate of the charged samples. It was found that the samples were heated from an ambient temperature to 852°C within 10 min. Then the samples were quenched in tap water. This procedure constituted a cycle. Experiments with samples exposed to one, two, three and four cycles were carried out aiming to verify the claim of Grange [8].

Metallographic examination/Image analysis

Five sets of specimen were prepared for metallographic examination. The procedure involved grinding the treated steel samples to produce a flat and smooth surface. Silicon carbide paper of different grades (220, 320, 400 and 600) placed on a grinding machine was used. Subsequently the samples were polished using a selvet cloth swamped with a solution of 1-micron and 0.5-micron silicon carbide to produce a mirror like surface. The samples were etched to reveal the boundaries of the polished surface using 2% Nital (2 % nitric acid and 98 % alcohol). Then they were washed, dried and viewed with an accuscope optical microscope at 400x magnification. The image analysis was carried out using Image J software following the flowchart in Fig. 1 [19, 26]. The grain sizes were determined by the planimetric method in accordance with ASTM E112-13 [27].

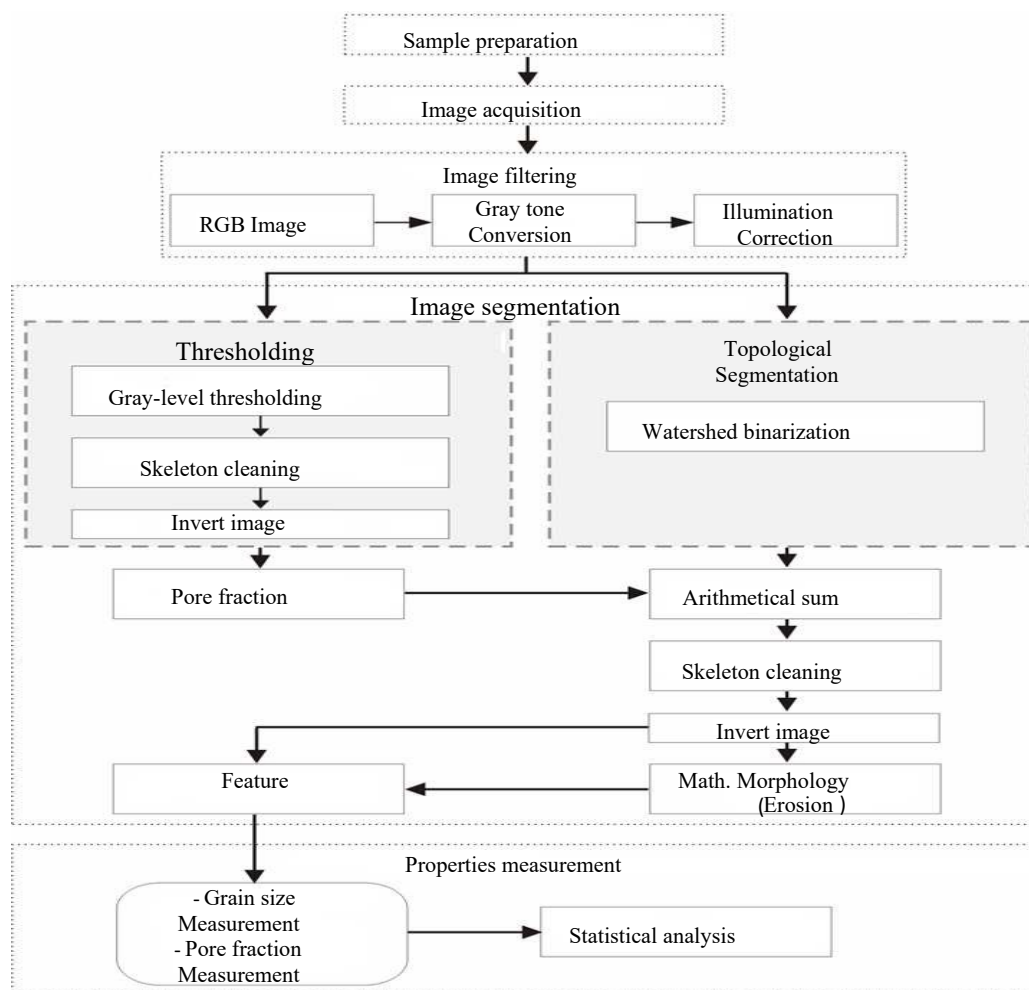


Fig. 1. Flowchart of Image J process [13].

Mechanical properties

The Brinell hardness was determined using Brinell hardness tester in accordance with ASTM E10-15 [28] standard. The Impact test was carried out using Charpy V-notch impact tester according to ASTM A370-10 [29] standard while the ultimate tensile test was conducted on an universal testing machine following ASTM E8 [30]. All mechanical properties were evaluated electronically. Three samples were used for each cycle and the corresponding average values were obtained.

RESULTS AND DISCUSSION

Heating and cooling rates

The diffusional heat treatment curve is presented in Fig. 2. The value of the heating rate of the initial diffusional heat treatment is equal to $15.90^{\circ}\text{C}/\text{min}$. Based on the assertion of Twiggs et al. [10], a heating rate less than $20^{\circ}\text{C}/\text{min}$ corresponds to slow heating. Hence, the heating used in this study is categorized as a slow one. Therefore, it is expected that complete austenitization of the steel [24, 25] will be achieved. Fig. 3 shows the cooling curve. The cooling rate at the quenching start

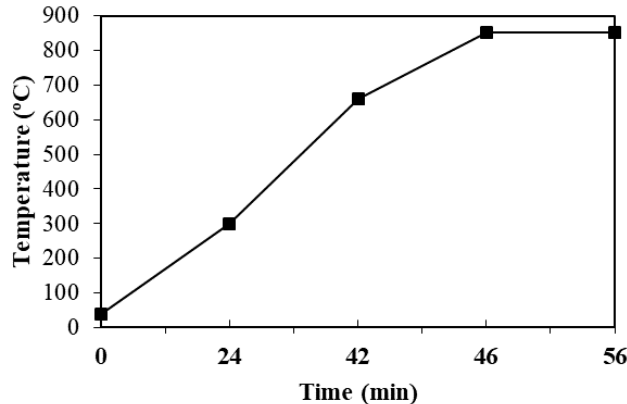


Fig. 2. Diffusional heating curve.

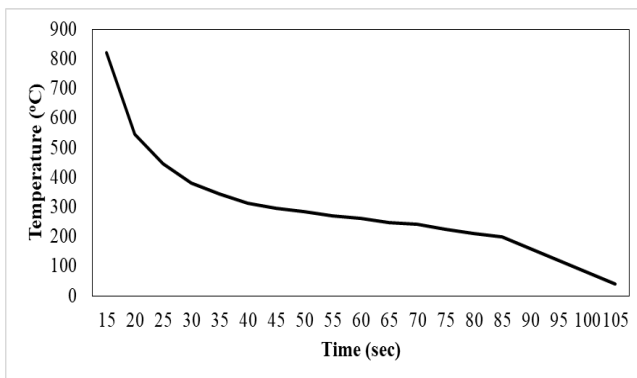


Fig. 3. Cooling curve for diffusional heat treatment.

is equal to $54.98^{\circ}\text{C}/\text{s}$. This implies that the cooling is rapid leading [31, 32] to a martensic microstructure at a room temperature. Fig. 4 shows the schematic representation of a cyclic rapid heating process. The heating rate obtained amounts to $84^{\circ}\text{C}/\text{min}$. This implies that the heating process is fast [10]. The possibilities of grain size refinement via this process are high [33].

Image analysis

Fig. 5 shows the microstructural images of the samples. The samples subjected to rapid cooling from its austenitic temperature to a room temperature attain a martensite microstructure [25, 31 - 32]. This is so because the fast cooling rate does not provide carbide particles even diffusion into the iron matrix. This results in jamming of the carbon lattice of the ferrite atomic arrangement. Martensite is therefore an aggregate of ferrite and cementite [34].

The martensite grains are very coarse. This determines the mottled contrast of Fig. 5(a). The black areas of the microstructures refer to the carbide particles [35]. They are greater in number in the control sample. The black areas decrease in the course of the treatment applied giving room to a finer microstructure of improved mechanical properties referred by Grange [8] to a fine martensite. Figs. 5(b), 5(c), 5(d) and 5(e) illustrate one cycle, two cycles, three cycles and four cycles of a rapid heat treatment, respectively. The treatment applied provides direct transformation of some of the martensite particles to austenite without passing through the intermediate phases (this is called displacive transformation). The carbon particles however are given more room to diffuse out and realign. This leads to a more evenly

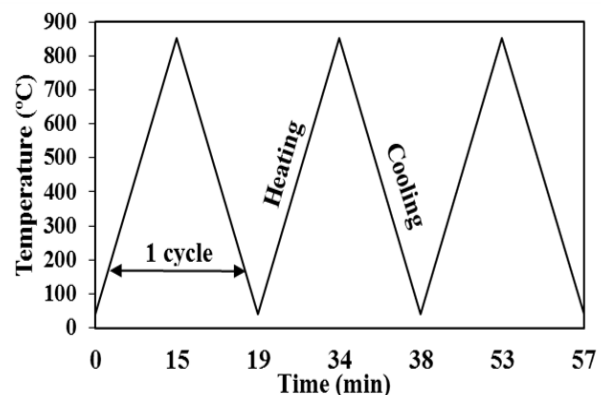


Fig. 4. Schematic representation of cyclic rapid heating process.

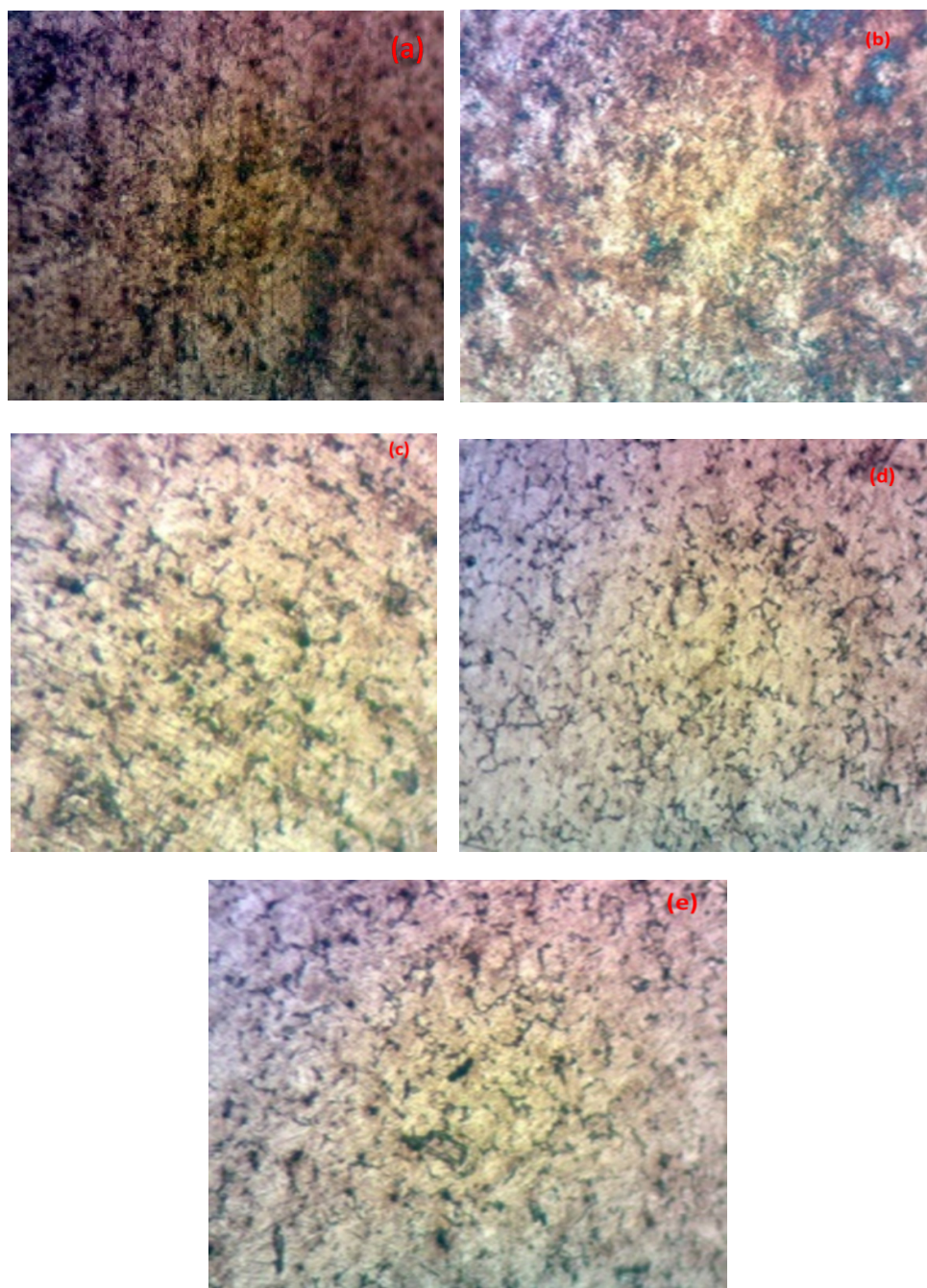


Fig. 5. Microstructure of samples at 400x magnification (a) control (b) one cycle (c) two cycles (d) three cycles (e) four cycles.

distributed microstructure on quenching. The process results in finer grains formation due to their nucleation and the corresponding boundaries formation [36]. According to Bhadeshia [33], the nucleation rate is accelerated by refining the austenite grain size as the density of nucleation sites increases inversely with the austenite grain size. The rapid heating prevents the growth of austenite grain size. Furthermore, the martensite microstructure

gets refined on quenching and the mottled contrast of Fig. 5(a) gradually becomes brighter.

Fig. 6 shows the threshold (black and white) view of the microstructures. The black areas refer to the carbide particles. They are most visible as clusters in case of the control sample (Fig. 6(a)) and the one-cycle sample (Fig. 6(b)), while the two-cycle sample (Fig. 6(c)) shows fewer clusters of carbide particles in the iron matrix.

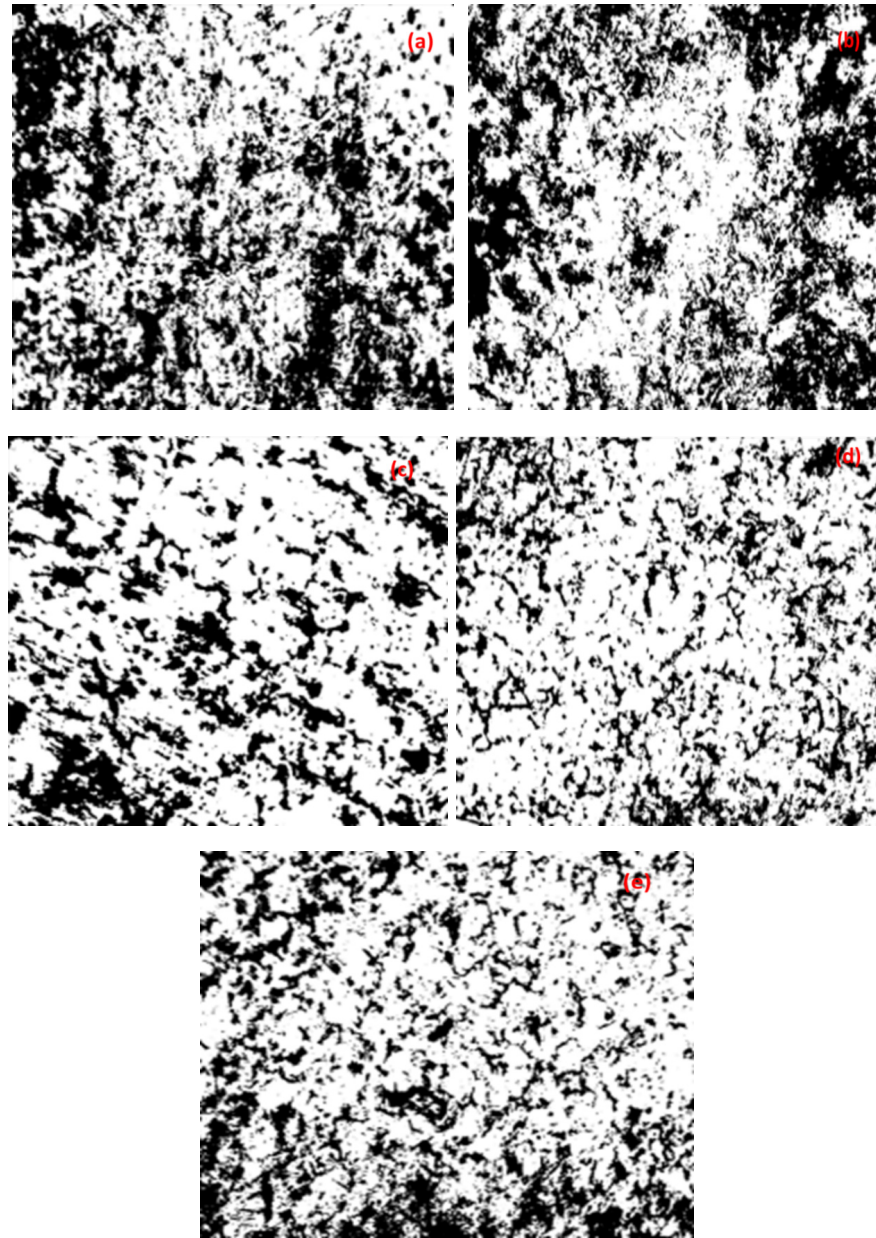


Fig. 6. Threshold view of microstructures (a) control (b) one cycle (c) two cycles (d) three cycles (e) four cycles.

There is a progressive increase of these black spots in the three- (Fig. 6(d)) and four-cycle samples (Fig. 6(e)). This shows that after two cycles of rapid heating, a jamming of carbide particles starts to form again in the selected mild steel sample. This trend is also evident in Fig. 7 which displays the map drawing of the microstructure. It indicates that the two-cycle sample (Fig. 7c) has a more even mixture of carbide and ferrite particles.

Fig. 8 shows the area count of the microstructures. The effect of several cycles of rapid heating is evident as the mean area of the samples decreases from 28.45

μm^2 in the control sample to 27.89 μm^2 in the two-cycle sample. It increases to 29.26 μm^2 in the four-cycle sample. It is evident that the two-cycle sample has the smallest average area. It is worth adding that two cycles of rapid heating result in a decrease of the grain area of the selected steel sample, while the further cycles lead to a corresponding increase of the grain area.

Fig. 9 displays the surface plot (3D view) of the microstructure. It shows that green portions revealing (Fig. 9(a)) a cluster of carbide particles which do not align properly in the iron matrix dominate the control

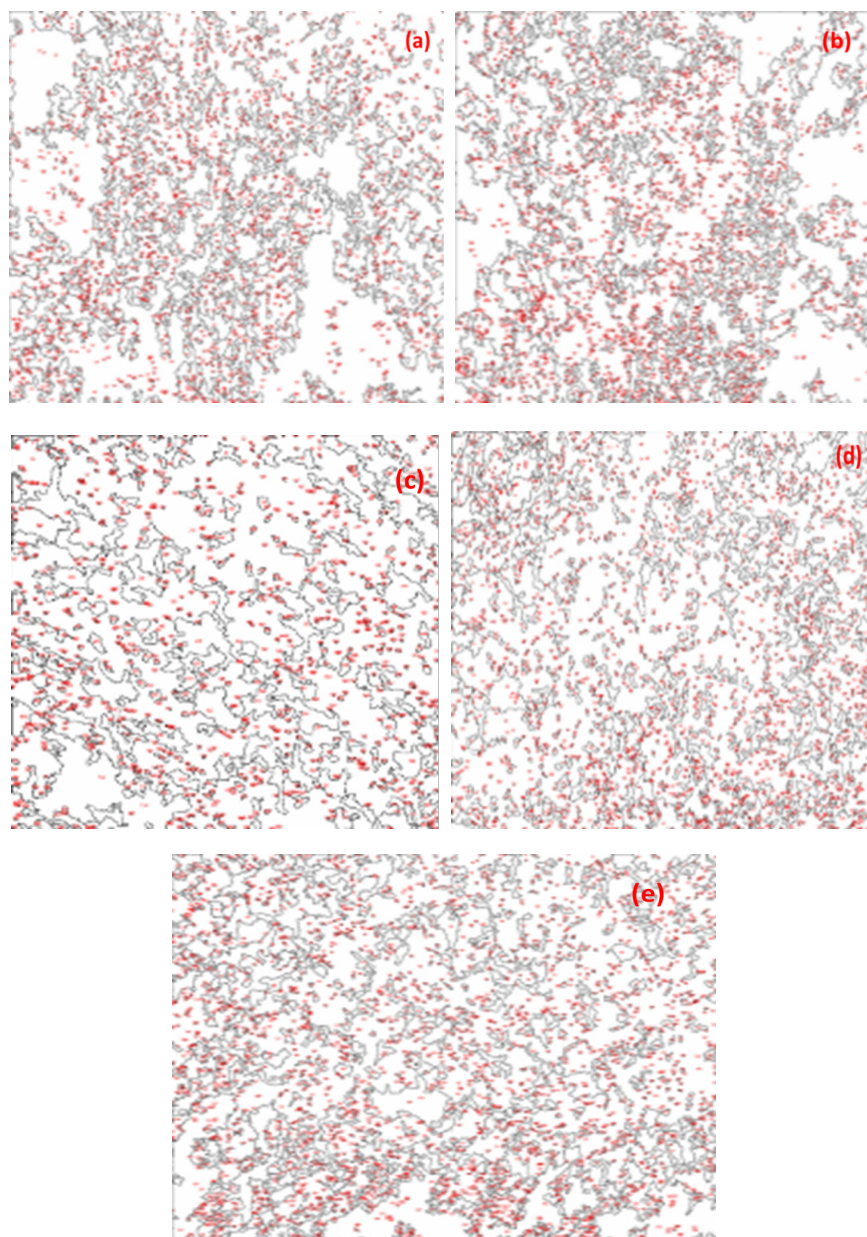


Fig. 7. Map (drawing) of microstructure (a) control (b) one cycle (c) two cycles (d) three cycles (e) four cycles.

sample. These green portions are gradually replaced by pink and blue one in the one-cycle sample plot (Fig. 9(b)) indicating the gradual realignment of the particles in the martensite matrix. After two cycles of a rapid treatment, most of the green portions observed in Fig. 9(a) are replaced by a pink portion as shown in Fig. 9(c). This implies that there is an even distribution of the carbide particles in the iron matrix structure. Subsequent cycles of a rapid heating result in a reappearance of the green portion as shown in Figs. 9(d) and 9(e).

The values of the image analyses parameters are

presented in Table 3. The results show that the total area decreases from the control ($1153849 \mu m^2$) to the two-cycle sample ($249739 \mu m^2$) and increases for the four-cycle sample ($859164 \mu m^2$). Similarly, the circularity of the samples, which is a measure of how close an object is to a true circle [19], also decreases from the control sample ($0.801 \mu m$) to the two-cycle one ($0.769 \mu m$) and then increases to the four cycles sample ($0.799 \mu m$). The maximum ferret diameter often referred to as ferret diameter, represents the longest dimension of the particle independent of its angular rotation [37,

Table 3. Image analyses parameters of samples.

Sample	count	Total Area	Average Size	Perimeter	IntDen	Circularity
Control	2499	1153849	461.72	57.31	11739.70	0.80
1-cycle	2877	1152582	400.62	41.69	50569.19	0.80
2-cycles	970	249739	257.46	54.29	65653.04	0.77
3-cycles	2633	663536	252.01	52.73	64261.94	0.79
4-cycles	2980	859164	288.31	52.49	73519.07	0.80
Sample	Solidity	Feret	Feret X	Feret Y	Feret Angle	Min Feret
Control	0.856	12.86	890.21	719.91	108.63	7.58
1-cycle	0.853	11.87	864.02	765.07	109.17	6.83
2-cycles	0.843	15.37	481.31	439.31	114.44	8.47
3-cycles	0.854	14.52	973.41	760.49	108.03	8.42
4-cycles	0.856	13.09	900.01	742.14	107.54	7.26

*The unit of Feret, Feret X, Feret Y, Min Feret, perimeter, IntDen and average size is μm ; total area is μm^2 while the unit of Feret angle is degree.

38). The ferret diameter varies from 12.957 μm in the control sample to 15.374 μm in the two-cycle sample. It is also observed that ferret X, ferret Y, ferret angle and minimum ferret vary in a similar pattern.

Fig. 10 displays the pictorial view of the samples grain size. It is evident that there is a decrease of the grain size from 1.07 μm in the control sample to 0.79 μm in the three-cycle one. However, there is an increase of the grain size of the four-cycle sample which shows that the further cycles of the rapid heat treatment will not lead to production of smaller grains.

Mechanical properties of the sample

Table 4 displays the mechanical properties of the

samples. It is evident that the two-cycle sample has the lowest Young modulus value (15.36 GN/m²). This indicates that it is the most ductile sample among the tested one because ductile materials usually exhibit low Young modulus values according to Callister [39]. The ultimate tensile strength decreases from 1.25 GN/m² in the control sample to 0.83 GN/m² in the two-cycle one and increases to 27.77 GN/m² in the four-cycle sample. This implies that the ultimate strength of the material decreases with the ductility increase. The results also reveal that there is an increase of the Brinell hardness number – it changes from 271 in case of the control sample to 562.7 for the four-cycle one. Similarly, the impact energy increases from 46.8 J for the control sample to

Table 4. Mechanical properties of samples.

Samples	YM (GN/m ²)	UTS (GN/m ²)	BHN	IE (Joules)	EA (N.m)
Control	22.65	1.25	271.00	46.80	230.98
1-Cycle	16.40	1.03	284.00	51.20	296.17
2-Cycles	15.36	0.83	323.00	55.40	235.15
3-Cycles	20.61	1.11	377.70	61.50	265.99
4-Cycles	27.77	1.32	562.70	64.60	253.65

*YM-Young Modulus, UTS - Ultimate Tensile Strength, BHN - Brinell hardness number, IE-Impact Energy, EA- Energy Absorbed.

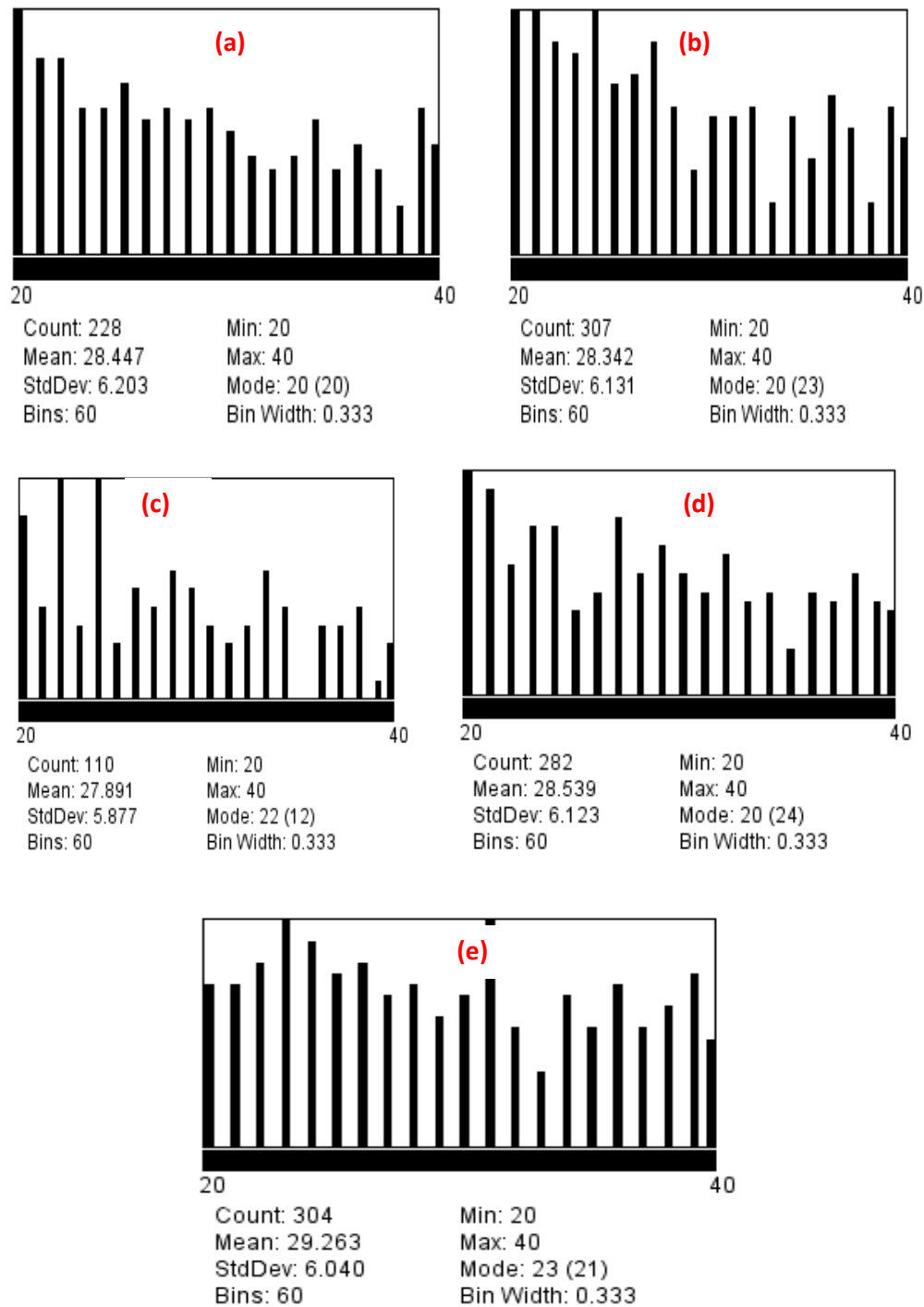


Fig. 8. Area of microstructures (a) control (b) one cycle (c) two cycles (d) three cycles (e) four cycles.

64.6 J for the four-cycle one. This indicates that the rapid cyclic heating increases mild steel hardness and impact energy. The results also show that the one-cycle sample absorbs the greatest energy (296.17 J) prior to a failure.

This implies that the one-cycle sample has the greatest toughness because materials of good toughness absorb more energy to fail. It has also a good combination of ductility and ultimate strength [40].

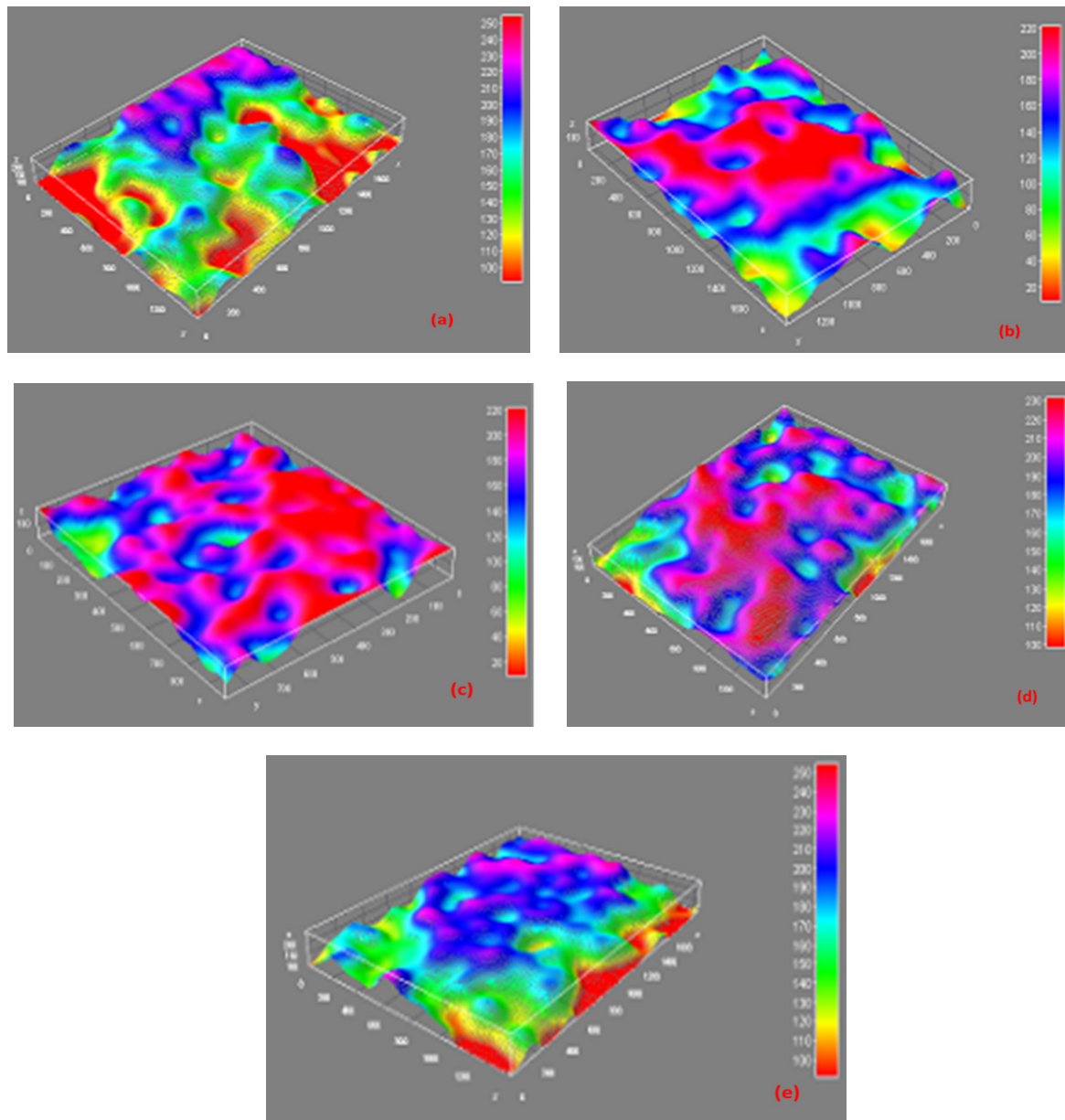


Fig. 9. Surface plot of microstructures (a) control (b) one cycle (c) two cycles (d) three cycles (e) four cycles.

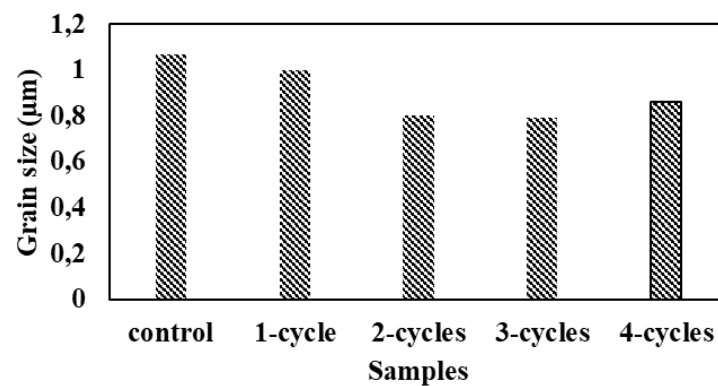


Fig. 10. Grain size of samples.

CONCLUSIONS

The present study is carried out to analyze the effect of the cyclic rapid heat treatment on mild carbon steel using an image analysis of its microstructure and mechanical properties. It is found that there is an improvement of the microstructure of the treated samples when compared to that of the control one. However, there is a marginal difference in the two-cycle and three-cycle samples with respect to the grain size which is equal to 0.8 μm and 0.79 μm , respectively.

The four-cycle sample shows a considerable increase of the grain size (0.86 μm). It can therefore be concluded that two cycles of a rapid heat treatment is optimal to produce fine grains in mild carbon steel. The mechanical properties of the mild steel sample are also improved.

Acknowledgements

The authors wish to acknowledge the guidance of Dr. Alo, F.I. of the Department of Metallurgical Engineering, Obafemi Awolowo University, in the course of the experiments carried out, especially those referring to the image analysis. The authors also acknowledge the contribution of Mr. Duniya of the Department of Agricultural Engineering University of Ilorin for granting access to their equipment.

REFERENCES

1. K. Muszka, J. Majta, L. Bienas, Effect of grain refinement on mechanical properties of micro-alloyed steels, *Metall. Found. Eng.*, 32, 2, 2006, 87-97.
2. B. Jiang, L. Yazheng, Microstructural characterization, strengthening and toughening mechanisms of quenched and tempered steel: Effect of heat treatment parameters, *Mat. Sci. Eng., A* 707, 2017, 306-314.
3. D. Jinlong, Examination of the effects of TiN Particles and grain size on charpy impact transition temperature in Steels, Master's thesis, University of Birmingham, U.K., School of Metallurgy and Materials, 2011.
4. T. Santhikumar, T.K. Ajiboye, Effect of heat treatment process on the mechanical properties of medium carbon steel, *J. Min. Mat. Characteriz. Eng.*, 11, 2, 2012, 143-152.
5. W. Chunfang, W. Maogu, S. Jie, H. Weijun, D. Han, Effect of microstructure refinement on the strength and toughness of low alloy martensitic steel, *J. Mat. Sci. Techn.*, 23, 5, 2006, 659-664.
6. R. Tejas, What is grain refinement? Available at <https://www.quora.com/what-isgrain-refinement>; 2016. (Accessed November 17th, 2016).
7. J. Adamczy, A. Grajcar, Heat treatment and mechanical properties of low-carbon steel with dual-phase microstructure, *J. Achiev. Mat. Manufact. Eng.*, 22, 2, 2007, 13-20.
8. R. A. Grange, The rapid heat treatment of steel. *Metall. Trans.*, 2, 1, 1971, 65-78.
9. D. Dabkowski, L.F. Porter, Method for effecting the rapid-treatment of steel plate, US 3692591 A, Published by United States Patent Office, Sept. 19, 1972.
10. S.W. Twigg, R.D. Ringie, R. Morena, C.W. Fairhurst, Glass transition temperatures at rapid heating rates, *J. Am. Cer. Soc.*, 68, 2, 1985, 58-59.
11. C. Böhne, A. Pyzalla, W. Reimers, Residual stresses due to laser surface treatment of a high nitrogen steel, Hahn Meitner Institute, Berlin, Germany, 2000.
12. C. Nowill, Investigation of quench and heating rate sensitivities of selected 7000 series aluminium alloys: A thesis in Materials Science Engineering (Master's thesis). Worcester Polytechnic Institute, USA, 2007.
13. M. Calcagnotto, D. Ponge, Y. Adachi, D. Raabe, Effect of grain refinement on strength and ductility of dual-phase steels, *Proceedings of the 2nd International Symposium on Steel Science*, Kyoto, Japan, 2009.
14. A.L. Gloanec, G. Billota and M. Gerland, Deformation mechanism in TiNi shape memory alloy during cyclic loading. *Mat. Sci. Eng. A*, 564, 2012, 351-358.
15. J.D. Beckley, D.R. Wilder, Effects of cyclic heating and thermal shock of hafnia stabilized with calcia, magnesia and yttria, Federal Scientific and Technical Information, Springfield, Virginia, USA, 1968.
16. A. Koscielna, S. Wojciech, Effect of cyclic heat treatment parameters on the grain refinement of Ti-48Al-2Cr-2Nb alloy, *Mat. Characteriz.*, 60, 2009, 1158-1162.
17. H. Lin, T. Lui, L. Chen, Effect of maximum temperature on the cyclic heating-induced embrittlement of high-silicon ferritic spheroidal-graphite cast iron,

- Mat. Trans., 45, 2, 2004, 569-576.
18. Z. Lv, Z. Ren, Z. Li, Z. Lu, M. Gao, Effect of two different cyclic heat treatments on microstructure and mechanical properties of Ti-V microalloyed steel, *Mat. Res.*, 18, 2, 2015, 304-312.
 19. F.I. Alo, E.O. Ajoge, M.O. Kunle, D.A. Isadare, A.A. Oyedele, G. Emordi, Comparison of image J analysis of structure of two constructional steel. *Am. J. Eng. Appl. Sci.*, 11, 1, 2018, 318-326.
 20. B. Katarma, R. Gajza, Quantification of microstructural parameter ferritic-martensite dual phase steel by image analysis, *Metal.*, 19, 2009, 1-6.
 21. B. Onyekpe, *The Essentials of metallurgy and materials engineering*, Ambik Press, Benin City, Nigeria, 2002.
 22. K.J. Sanjib, Heat treatment of low carbon steel: A project report in Mechanical engineering., National Institute of Technology, Rourkela, India, 2009 [Undergraduate Thesis].
 23. S. Park, ME 3701: Materials laboratory, Louisiana State University, LA, USA, 2013.
 24. F.L.G. Oliveira, M. Andrade, A.B. Cota, Kinetics of austenite formation during continuous heating in a low carbon steel, *Mat. Characteriz.* 58, 2007, 256-261.
 25. J.L. Dosselt, H.E. Boyer, *Practical heat treating*, ASM International, USA, 2006.
 26. A.N. Diógenes, C.P. Fernandes, E.A. Hoff, Grain size measurement by image analysis: An application in the ceramic and in the metallic industries, *Proceedings of the 18th International Congress of Mechanical Engineering*, Ouro Preto, Brazil, 2005.
 27. ASTM E112-13, Standard Test Methods for Determining Average Grain Size, ASTM International, West Conshohocken, PA, 2013, www.astm.org
 28. ASTM E10-15, Standard Test Method for Brinell Hardness of Metallic Materials, ASTM International, West Conshohocken, PA, 2015, www.astm.org
 29. ASTM A370-10, Standard Test Methods and Definitions for Mechanical Testing of Steel Products, ASTM International, West Conshohocken, PA, 2010, www.astm.org
 30. ASTM E8 / E8M-13, Standard Test Methods for Tension Testing of Metallic Materials, ASTM International, West Conshohocken, PA, 2013, www.astm.org
 31. T. Guarav, Notes on material science, Materials Engineering Department AKGEC, GZB, 2015.
 32. E.T. Akinlabi, S.A. Akinlabi, Characterising the effects of Heat treatment on 3CR12 and AISI316 Stainless Steels, *Int. J. Mech. Aero. Ind. Mechat. Manufac. Eng.*, 8, 2, 2014, 256-261.
 33. H.K.D.H. Bhadeshia, Very short and very long heat treatments in the processing of steel, *Mat. Manufac. Proc.*, 25, 2010, 1-6.
 34. M. Gebril, M. Suliman, A. Khblan, Effect of austenitization temperatures and times on hardness, microstructure and corrosion rate of high carbon steel, *Des. Comput. Mod. Eng. Mat. Adv. Struc. Mat.*, 54, 2014, 421-428.
 35. A. Todric, B. Pejovic, P. Korac, D. Jesic, B. Sakovic, Improvement of toughness and hardness of high alloyed steel by vanadium and appropriate heat treatment, *J. Prod. Eng.*, 8, 1, 2015, 13-17.
 36. C. Peng, Y. He, B. Huang, P.K. Liaw, Effects of rapid heat treatment on microstructures and compression mechanical properties of TiAl-based alloy, *Trans. Non-ferr. Metall. Soc.*, 4,3, 2004, 460-463.
 37. J. Bodycomb, J-Image analysis: evaluating particle size shape. Available at www.horiba.com/us/particle; 2011. Accessed on 7th Jan., 2019.
 38. C. Shitanthi, R.K. Porpatham, N. Pappa, Image analysis for particle size distribution. *International Journal of Engineering and Technology*, 2014, 1340 – 1344.
 39. W.D. Callister, *Materials Science and Engineering- An Introduction*, 6th ed., John Wiley & Sons, Inc., 2007.
 40. NDT Resource Centre, Mechanical properties, Available at <https://www.ndeet.org/EducationResources/CommunityCollege/Materials/Mechanical/Mechanical.htm>. Accessed on October 13th, 2016.